Available online at www.sciencedirect.com
SCIENCE DIRECT®
PHYSICS LETTERS B
ELSEVIER
Physics Letters B 556 (2003) 114–122
www.elsevier.com/locate/npe

The dipole picture and saturation in soft processes

J. Bartels [a], E. Gotsman [b,c], E. Levin [b,c], M. Lublinsky [c], U. Maor [b]

[a] *II Institut für Theoretische Physik, Universität Hamburg, D-22761 Hamburg, Germany*
[b] *HEP Department, School of Physics and Astronomy, Raymond and Beverly Sackler Faculty of Exact Science, Tel Aviv University, Tel Aviv 69978, Israel*
[c] *DESY Theory Group, 22607 Hamburg, Germany*

Received 19 December 2002; accepted 22 January 2003

Editor: P.V. Landshoff

Abstract

We attempt to describe soft hadron interactions in the framework of saturation models, one based upon the Balitsky–Kovchegov non-linear equation and another one due to Golec-Biernat and Wüsthoff. For pp, Kp, and πp scattering the relevant hadronic wave functions are formulated, and total, elastic cross-sections, and the forward elastic slope are calculated and compared to experimental data. The saturation mechanism leads to reasonable reproduction of the data for the quantities analyzed, except for the forward elastic slope, where the predicted increase with energy is too moderate.

1. Introduction

Understanding the high energy behaviour of total hadronic cross-sections within the framework of QCD is one of the intriguing problems of high energy physics. The main difficulty lies in the fact that presently most applications of QCD are based on perturbation theory which is only applicable for "hard" processes (i.e., it needs a "hard" scale), while hadronic processes near the forward direction are "soft" and non-perturbative by definition. On the other hand, the past few years have seen much activity in the successful application of QCD to DIS processes. For values of $Q^2 \geqslant 2$ GeV^2, the use of perturbative QCD seems to be trustworthy. For very small Q^2 one can rely on Regge theory (e.g., [1]) which provides a reasonable description of the data. The construction of a very promising bridge between these two theoretical frameworks has been pioneered by the concept of high parton densities and saturation. Models based upon this idea have been successful in describing the DIS cross-section for all values of Q^2 and energies $x \leqslant 0.01$. [2–4].

The goal of this Letter is an attempt to apply the dipole picture and the physics of high parton densities to soft hadronic cross-sections. We want to explore to what extent the high energy hadronic asymptotic behaviour can be explained by the saturation hypothesis, which—so far—has been tested in the context of deep inelastic scattering at small x and in γ–γ

E-mail addresses: jochen.bartels@desy.de (J. Bartels), gotsman@post.tau.ac.il (E. Gotsman), leving@post.tau.ac.il, levin@mail.desy.de (E. Levin), lublinm@mail.desy.de, mal@tx.technion.ac.il (M. Lublinsky), maor@post.tau.ac.il (U. Maor).

0370-2693/03
doi:10.1016/S0370-2693(03)00128-X

scattering. The idea of saturation concerns the interactions between partons from different cascades, which in the linear evolution equations (DGLAP and BFKL) are not included, and which become more important with increasing energy. The parton saturation phenomenon then introduces a characteristic momentum scale $Q_s(x)$, which is a measure of the density of the saturated gluons. It grows rapidly with energy, and it is proportional to $\frac{1}{x^\lambda}$ [5–7] with $\lambda \simeq 0.2$. Parton saturation effects are expected to set in at low values of Q^2 and x, where the parton densities are sufficiently large.

At this stage we do not discern how to relate the dipole picture to the additive quark model which has been successful in explaining and relating different hadronic total cross-sections. Instead, we consider this study as being exploratory, and we will not attempt to draw any conclusions concerning this rather fundamental issue.

The basis of our endevour is the successful fit [4] to the F_2 structure function data for all values of Q^2 and $x \leqslant 0.01$, within the framework of QCD, achieved by using an approximate solution to the Balitsky–Kovchegov (BK) [8] non-linear evolution equation, and adding a correcting function to improve the DGLAP behaviour at large Q^2. Although soft physics is not explicitly included, agreement with experiment is found for all parameters associated with F_2, in particular for the logarithmic slope $\lambda \equiv \partial \ln F_2/\partial(\ln 1/x)$, a value of $\lambda \approx 0.08$ was obtained at very low x and Q^2 well below 1 GeV^2, i.e., in the saturation region. This agrees with the value of the intercept of the "soft" pomeron, associated with the Donnachie–Landshoff (DL) model [9].

In this Letter we start from the hypothesis that also in hadron–hadron scattering at high energies color dipoles might be the correct degrees of freedom, even when large transverse distances come into play. We start from the well known expression for DIS cross-sections

$$\sigma_{T,L}^{\gamma^* p}(x, Q^2) = \int d^2 r_\perp \, dz \left|\psi_{T,L}(Q, r_\perp, z)\right|^2 \sigma_{\text{dipole}}(x, r_\perp), \tag{1.1}$$

where Q^2 denotes the virtual photon's four momentum squared, $\psi_{T,L}$ its wave function, W^2 the energy squared in the photon–proton system and z, $(1-z)$ the momentum fraction taken by the quark (antiquark) respectively. $r_\perp$ is the transverse distance between the q and $\bar{q}$, and $x = \frac{Q^2}{(W^2+Q^2)}$. There are two main elements in Eq. (1.1): (a) the wave function of the virtual photon, and (b) the dipole cross-section, which describes the interaction of the $q\bar{q}$ with the proton target, through the exchange of a gluon ladder. In the DIS case the wave function for the virtual photon is well known, whereas for the hadron case this is not so. We discuss the question of the hadronic wave functions in Section 3.

It would be naive for us to expect that our treatment is able to yield the complete hadronic cross-section. We have, at least, two reasons for this statement: first, at large impact parameter we have to include the non-perturbative contributions even for the so-called "hard" processes [10–12] since this behaviour is defined by the spectrum of hadrons [13]; second, at present the impact parameter dependence of the interaction is only treated approximately. In [2], the dipole cross-section has a built-in sharp cutoff in b at the value of the proton radius; in other cases [4] the equation is first solved for $b = 0$, and then an ansatz is made regarding factorization and the assumed b dependence of the dipole cross-section. For hadronic interactions the impact parameter dependence is known to be important, and neither a sharp (in particular: energy independent cutoff) nor the method of calculating saturation at $b = 0$, and assuming that the b-shape does not change with energy, is, at best, a very rough approximation to the physical situation.

The content of the Letter is as follows. In Section 2 we discuss the numerical solution of the BK equation [8], and the changes that must be made to adapt this for the calculation of hadron–hadron cross-sections. In Section 3 we present the details of our calculation. Section 4 is devoted to the overall picture, including comparison of the model predictions with experimental data. Section 5 contains a discussion of our results and our conclusions. In Appendix A we explain why the results for the forward elastic slope are so shallow.

2. The master equation

In [4] an approximate solution to the BK non-linear evolution equation [8] was obtained using numerical

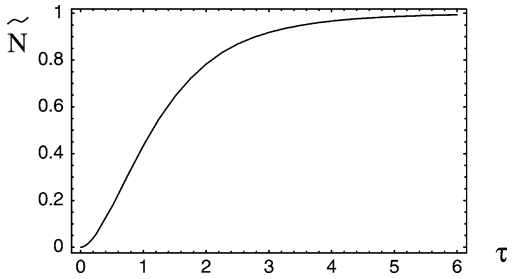

Fig. 1. $\widetilde{N}(b=0)$ versus $\tau = r_\perp Q_s(x)$.

techniques. Below we briefly review the method used and the main results obtained. For more details of the method of solution we refer to [4].

The solution of the BK equation which we denote by $\widetilde{N}$, takes into account the collective phenomena of high parton density QCD. Starting from an initial condition which contains free parameters we have numerically solved the non-linear evolution equation, restricting ourselves to the point $b = 0$. The parameters have been fitted to the F_2 data [4], and the resulting approximate solution is displayed in Fig. 1.

The b-dependence of the solution is restored using the ansatz:

$$\widetilde{N}(r_\perp, x; b) = \bigl(1 - e^{-\kappa(x,r_\perp)S(b)}\bigr), \tag{2.1}$$

where κ is related to the $b = 0$ solution

$$\kappa(x, r_\perp) = -\ln\bigl(1 - \widetilde{N}(r_\perp, x, b=0)\bigr). \tag{2.2}$$

The Gaussian form for the profile function in impact parameter space was assumed, i.e.,

$$S(b_\perp) = \frac{1}{\pi R^2_{\text{proton}}} \exp\biggl(-\frac{b^2_\perp}{R^2_{\text{proton}}}\biggr), \tag{2.3}$$

where $R^2_{\text{proton}} = 3.1\ \text{GeV}^{-2}$ refers to the radius of the target proton. The dipole–proton cross-section (from Eq. (2.4) of [4]) is given by:

$$\sigma_{\text{dipole}}(r_\perp, x) = 2\int d^2b_\perp\, \widetilde{N}(r_\perp, b_\perp, x). \tag{2.4}$$

Another popular saturation model was proposed by Golec-Biernat and Wüstoff [2] which we will denote by GBW. The following dipole cross-section is assumed to be:

$$\hat{\sigma}(r_\perp, x)_{\text{dipole}} = \sigma_0\biggl[1 - \exp\biggl(-\frac{r^2_\perp}{4R^2_0}\biggr)\biggr] \tag{2.5}$$

with $R^2_0(x)[\text{GeV}^{-2}] = (\frac{x}{x_0})^\lambda$. The values of the parameters which were determined by fitting to DIS data at HERA for $x \leqslant 0.01$, are: $\sigma_0 = 23$ mb, $\lambda = 0.29$ and $x_0 = 3 \times 10^{-4}$. The $r_\perp$ dependence is taken as Gaussian, which leads to a constant cross-section σ_0 for large $r_\perp$ (or small Q^2), i.e., for "soft" interactions.

The dipole cross-section of the GBW saturation model and $\widetilde{N}$ are closely related. Both models include the effects of gluon saturation, preserve unitarity, and describe the physics associated with "long distances". Whereas $\widetilde{N}$ has some support from QCD, $\hat{\sigma}_{\text{dipole}}$ of the GBW model has more the character of a phenomenological model.

Unlike the GBW $\hat{\sigma}_{\text{dipole}}$, the dipole cross-section obtained from the solution of the BK equation is not saturated as a function of x. This emanates from the integration over b. With the assumed Gaussian profile function it leads to a logarithmic growth with decreasing x. The Froissart-like behaviour $\sigma_{\text{dipole}} \propto \ln^2(1/x)$ [13] is crucially dependent on the fact that the large impact parameter behaviour of the dipole cross-section is exponential, rather than Gaussian.

Starting from our dipole cross-sections we obtain our master equation for the hadron–proton cross-section

$$\sigma_{H-\text{proton}}(x) = \int d^2r_\perp \bigl|\psi_H(r_\perp)\bigr|^2 \sigma_{\text{dipole}}(r_\perp, x), \tag{2.6}$$

where $\psi_H(r_\perp)$ represents the wave function of the hadron which scatters off the target proton. The form taken for $\psi_H(r_\perp)$ is discussed in the next section.

For both saturation models ((2.4) and (2.5)) the energy dependence of the hadron–proton cross-section enters only through x-dependence of the dipole cross-section, the latter being adjusted or constructed to describe DIS data of the F_2 structure function. The way in which the x-dependence of the dipole cross-section determines the energy dependence of the hadron cross-sections is strongly influenced by the b-slope. Note, however, that there is no x in hadron–hadron collisions. In order to relate x to the energy of the process we will need to introduce an additional non-perturbative scale, denoted below as Q^2_0.

3. Details of calculation

3.1. Hadronic wave function

There is no established method for calculating hadronic wave functions within the framework of QCD. The Heidelberg group Dosch et al. [14] using the stochastic vacuum model, have calculated hadronic cross-sections, after making an ansatz regarding the form of the hadronic wave function $\psi_H(r)$. We adopt their ansatz and utilize hadronic wave functions of similar shape to those used in [14].

Based on experimental evidence of the flavour dependence of hadronic cross-sections, which decrease with increasing number of strange quarks, the authors of [14] hypothesized that the cross-sections depend on the sizes of the hadrons in the process.

For the hadron transverse wave function we take a simple Gaussian form, the square of the wave function is given by

$$\left|\psi_M(r_\perp)\right|^2 = \frac{1}{\pi S_M^2}\exp\left(-\frac{r_\perp^2}{S_M^2}\right), \tag{3.1}$$

where S_M is a parameter related to the meson size. We have used $S_\pi = 1.08$ fm and $S_K = 0.95$ fm. These S_M were found from experimental values for the electromagnetic radii, namely, $R_\pi = 0.66 \pm 0.01$ fm and $R_K = 0.58 \pm 0.04$ fm [15]. For meson wavefunction of the form (3.1) $S_M = \sqrt{\frac{8}{3}}R_M$.

The proton's wave function squared is given by

$$\left|\psi_p(r_{1\perp}, r_{2\perp})\right|^2 = \frac{1}{(\pi S_p)^2}\exp\left(-\frac{r_{1\perp}^2 + r_{2\perp}^2}{S_p^2}\right), \tag{3.2}$$

where $S_p = 1.05$ fm, which corresponds to $R_p = 0.862 \pm 0.012$ fm [15]. For proton wave function of the form (3.2) $S_p = \sqrt{\frac{3}{2}}R_p$.

For meson–proton scattering, the meson is treated as a quark–antiquark pair (i.e., a colour dipole), and therefore the calculation follows that of DIS, i.e., the interaction of a colour dipole with a proton target, with the meson wave function replacing that of the virtual photon. However, for the scattering of a baryon projectile, we represent the baryon as constituted of two colour dipoles, one dipole formed around two quarks, and the second dipole from the center of mass of these two quarks to the third quark in the baryon. Generally speaking the parameter S_p in (3.2) can be different for these two dipoles. For example, in the non-relativistic additive quark model (AQM) we expect S_p for the first dipole to be larger by the factor $4/3$ compared to the second dipole. In (3.2), for simplicity, they are choosen to be identical. It will be shown below that the hadron cross-sections are mostly determined by the saturation domain where the sensitivity to the wave function and, in particular, to the choice of S_p is quite weak.

In AQM, the $\frac{2}{3}$ ratio between $\pi-p$ and $p-p$ cross-sections is due to quark counting. In our model, at very high energies when the dipole cross-section is independent of the dipole size, the predicted ratio is $\frac{1}{2}$, given by the number of dipoles in the pion relative to those in the proton. In our approach the high energy interaction is blind with respect to the flavours of the interacting quarks, and the ratio $\sigma_{\rm tot}^{Mp}/\sigma_{\rm tot}^{pp} = 1/2$, seems to disagree with the data. Experimentally, at an energy of $\sqrt{s} = 20$ GeV, $\sigma_{\rm tot}^{\pi p}/\sigma_{\rm tot}^{pp} \approx 0.6$. We expect the secondary Regge trajectories to give a smaller contribution to K^+p interaction, as there are no resonances in the s channel of this reaction, the same is also true for proton–proton scattering. The predicted ratio $\sigma_{\rm tot}^{K^+p}/\sigma_{\rm tot}^{pp} = 1/2$ is in reasonably good agreement with the experiment data.

3.2. Method of calculation

All the parameters in $N(r_\perp, b_\perp, x)$ were taken from the fit of

$$F_2\big(Q^2, x\big) = \frac{Q^2}{4\pi^2\alpha_{\rm elem}}\sigma^{\gamma^* p}\big(Q^2, x\big) \tag{3.3}$$

made to the experimental DIS data, (see [4] for details). In the DIS case the variable x is well defined in terms of Q^2 and W^2, in the hadronic case we redefine x to be $x = Q_0^2/s$, where s denotes the energy squared in the center of mass system of the hadrons, and Q_0^2 is a parameter which we adjust to be compatible with the data. The value of Q_0^2 is determined by the longitudinal part of the wave function, for which at present we do not have a reasonable model. In general we would expect the scale Q_0 to increase with increasing hadron masses, and thus vary from hadron to hadron. In this study we will fit this parameter separately for each projectile hadron.

In the colour dipole picture (which is equivalent to two gluon exchange), one can hopefully only reproduce the asymptotic energy dependence, i.e., the pomeron contribution. At lower energies where most of the data for meson baryon scattering is available, there are also contributions from secondary trajectories. The evaluation of these contributions is beyond the scope of our model.

4. Comparison of our model predictions with data

Our model contains a parameter Q_0^2, (which can be considered as a scale factor) from the definition of $x = \frac{Q_0^2}{W^2}$, in analogy with the variable in DIS, $x \approx \frac{Q^2}{W^2}$. The energy dependence of the hadronic cross-sections can be adjusted by choosing a suitable value for this variable. We found that the value $Q_0^2 = 3.5 \times 10^{-3}$ GeV^2, gives good agreement with the data for $\sigma_{\rm tot}(K^+p)$. See Fig. 2(a). The K^+p channel was chosen as it is exotic, having no resonances in s channel and therefore by duality the secondary Regge trajectory contributions are small. By replacing the wave function of the K^+ meson in Eq. (3.1) by that of the π meson, we obtain $\sigma_{\rm tot}$ for the π^-p. We display our prediction and the data in Fig. 2(a). We have chosen to show $\sigma_{\rm tot}(\pi^-p)$ compared to data, as there are more data in this channel than in the π^+p channel. The cross-sections σ_{π^+p} and σ_{π^-p} only differ due to the contribution of the secondary trajectories. The parameters used for $\sigma_{\rm tot}(\pi^-p)$ are $Q_0^2 = 1 \times 10^{-3}$ GeV^2, and a Regge contribution of $27 \times (\frac{s}{s_0})^{-0.45}$ mb ($s_0 = 1$ GeV^2) which has a smaller residue than that suggested by the DL model.

We note that the predicted energy dependence for $\sigma_{\rm tot}(\pi^-p)$ is more moderate than the data, and at an energy of $p_{\rm lab} = 400$ GeV, we underestimate the experimental data by approximately 7%.

We compare our results with those of the GBW model, by replacing $\sigma_{\rm dipole}$ in Eq. (2.6), by the GBW dipole $\hat{\sigma}(x, r_\perp)_{\rm dipole}$ given in Eq. (2.5). We wish to stress that the GBW saturation model was formulated for, and applied to DIS reactions [2]. The responsibility of extending the model to hadronic interactions is ours. The GBW model does not contain any explicit b-dependence, but one can consider the constant cross-section to be the result after integration over the impact parameter (with a sharp impact parameter cutoff put into the exponent in (2.5)). It is clear that at asymptotic energies (where one can neglect the contribu-

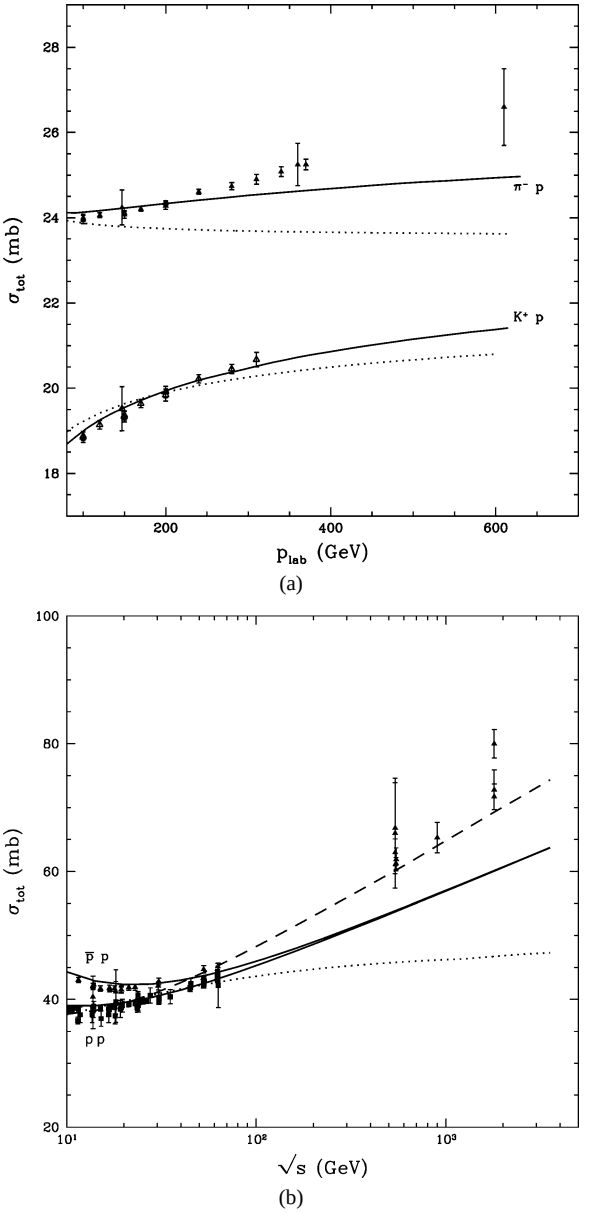

Fig. 2. (a) K^+p and π^-p total cross-sections. The full line is the prediction of our model and the dotted line using the Golec-Biernat Wüsthoff dipole. (b) $\bar{p}p$ and pp total cross-sections. The full lines are the model predictions with a Gaussian profile. The dashed line is the result of using a K_1 profile, and the dotted line using the Golec-Biernat Wüsthoff dipole. Data compilation from Ref. [16].

tion of secondary trajectories), the GBW cross-section for $\sigma_{\rm tot}(Mp) \leqslant 23$ mb, and $\sigma_{\rm tot}(Bp) \leqslant 46$ mb, as we have one (two) dipoles interacting with the proton target for Mp (Bp) scattering. In Fig. 2(a) we show the result (dotted line) obtained using the GBW form for the dipole Eq. (2.5) for the K^+p channel, with $Q_0^{2(\rm GBW)} = 0.27$ GeV^2, and using the same form of the hadronic wave function as discussed in Section 3.1. For $\pi^- p$ channel we used the almost maximal possible dipole cross-section, put $Q_0^2 = 5 \times 10^{-4}$ GeV^2, and add a secondary trajectory with $11 \times (\frac{s}{s_0})^{-0.45}$ mb. Due to the argument presented above, the GBW model cannot be adjusted to these data at all.

For $\sigma_{\rm tot}(\bar{p}p)$ (see Fig. 2(b)) the energy dependence predicted by the model is not as steep as the experimental data, yielding a value for $\sigma_{\rm tot}(\bar{p}p) \approx 65$ mb (instead of 72 mb) at Tevatron energies. I.e., a deficit of 10%, however, this is over a much wider energy range than in the $\pi^- p$ case. For $\sigma_{\rm tot}(pp)$ (where data is only available over a narrower range of energy) we achieve a very good reproduction of the experimental data, this is displayed in Fig. 2(b). For the pp and $p\bar{p}$ channels we take $Q_0^2 = 0.03$ GeV^2, and following [9] have a Regge contribution of $98.4 \times (\frac{s}{s_0})^{-0.45}$ mb for $\sigma_{\rm tot}(\bar{p}p)$ and $56 \times (\frac{s}{s_0})^{-0.45}$ mb for $\sigma_{\rm tot}(pp)$.

To get a handle on the theoretical uncertainties of our treatment we have also calculated $\sigma_{\rm tot}(\bar{p}p)$, using a profile function

$$S(b) = \frac{2}{\pi R_{\rm proton}^2}\left(\frac{\sqrt{8}\,b}{R_{\rm proton}}\right)K_1\left(\frac{\sqrt{8}\,b}{R_{\rm proton}}\right), \tag{4.1}$$

which corresponds to the Fourier transform of the "dipole" form factor in the momentum transfer representation:

$$F_{\text{"dipole"}}(t) = \left(1 - \frac{R_{\rm proton}^2 t}{8}\right)^{-2}. \tag{4.2}$$

The result of our calculations with the "dipole" form factor for $\sigma_{\rm tot}(\bar{p}p)$ is shown by the dashed line in Fig. 2(b). For this calculation we took $Q_0^2 = 0.06$ GeV^2. For the comparison with the F_2 data [4], a value of $R_{\rm proton}^2 = 4.46$ GeV^{-2} was used.

We repeat the same procedure for the $\bar{p}p$ channel for the GBW model as we did for $\sigma_{\rm tot}(K^+p)$ explained above, now with parameters $Q_0^{2(\rm GBW)} = 0.7$ GeV^2, and a Regge contribution of $20 \times (\frac{s}{s_0})^{-0.45}$ mb, (adjusted to the data), and taking the same form for the baryon wave function. The results are shown as a dotted line in Fig. 2(b).

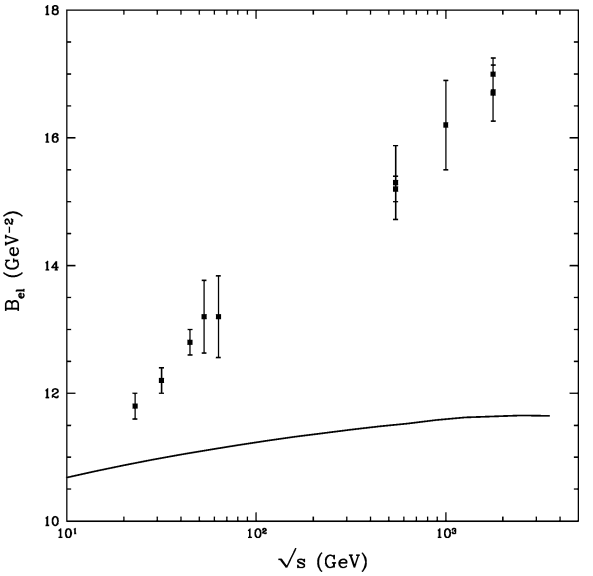

Fig. 3. $\bar{p}p$ forward elastic slope. Data compilation from Ref. [16].

We also calculate the forward slope of the elastic cross-section, i.e., B, which is defined as

$$\frac{d\sigma}{dt} = \left.\frac{d\sigma}{dt}\right|_{t=0} e^{-Bt}$$

and is related to the sizes of the particles participating in the reaction. $B = B_0 + B'$ where

$$B' = \frac{\int d^2r_\perp\, |\psi_H(r_\perp)|^2 b_\perp^2 N(r_\perp, b_\perp, x)\, db_\perp^2}{\sigma_{\rm tot}} = \frac{1}{2}\langle b_\perp^2\rangle. \tag{4.3}$$

Fig. 3 displays $B = B_0 + B'$ with $B_0 = 7.8$ GeV^{-2}. B_0 is related to the formfactors of the hadrons. Its value was chosen with an eye on the data, and is close to that used by Schuler and Sjöstrand [17].

The results we obtain are disappointing, but understandable and demonstrate the weak point of our model viz. the assumption of the oversimplified form for the impact parameter dependence of the amplitude (see Appendix A). The elastic slope (unlike $\sigma_{\rm tot}$) is sensitive to the $b_\perp$ distribution, and our assumption that the major contribution comes from small values of $b_\perp$ is obviously wrong. We will expand on this difficulty in Section 5 and Appendix A.

Using the relation

$$\sigma_{\text{elastic}} = \frac{(\sigma_{\text{tot}})^2}{16\pi B}$$

we check our model's predictions for σ_{elastic} for the $\bar{p}p$ channel, where the data extends to high energies. The model produces a very good description of the elastic $\bar{p}p$ cross-section (see Fig. 4(a)). In σ_{elastic}, the deficiency in the energy rise of σ_{tot} is to some extend compensated by the inadequacy of B.

We find it of interest to investigate how close we are to a black disc picture for dipole–proton scattering, which we do by utilizing the Pumplin bound [19], which follows from unitarity considerations and can be written as:

$$R_D = \frac{\sigma_{\text{elastic}} + \sigma_{\text{diff}}}{\sigma_{\text{tot}}} = \frac{\int d^2r_\perp d^2b_\perp |\psi_H(r_\perp)|^2 N^2(r_\perp, b_\perp, x)}{\sigma_{\text{tot}}} \leqslant \frac{1}{2}.$$

In Fig. 4(b) we display the ratio R_D and the experimental data. The model's predictions agrees with the data, and suggests that even at Tevatron energies we are 20% away from the black disc limit of $\frac{1}{2}$.

5. Discussion and conclusions

Our treatment has two parameters:

(a) R_h^2 which is taken from the electromagnetic radius of the hadron (following the Heidelberg prescription);
(b) the parameter Q_0^2, (introduced after Eq. (3.3), is adjusted by comparing with the data for the different channels. It is worth mentioning that, as expected, the obtained values for Q_0 reflect the mass hierarchy of the projectile hadrons.

In addition, we require the contribution of secondary trajectories at lower energies.

We would like to emphasis that our approximate solution to the BK equation [4] is obtained for impact parameter $b = 0$, and then an ansatz is made regarding the b dependence of the profile function $S(b)$. In the original fit to the F_2 data [4], $S(b)$ was taken to be a Gaussian, (which is equivalent to assuming that the dependence upon t, the momentum transfer squared,

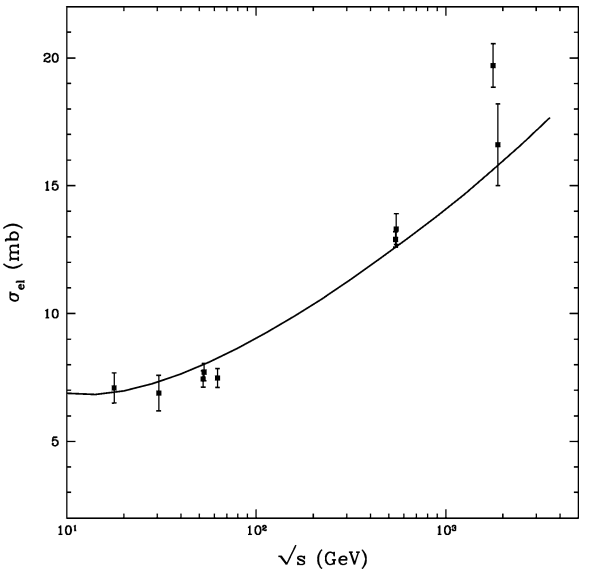

(a)

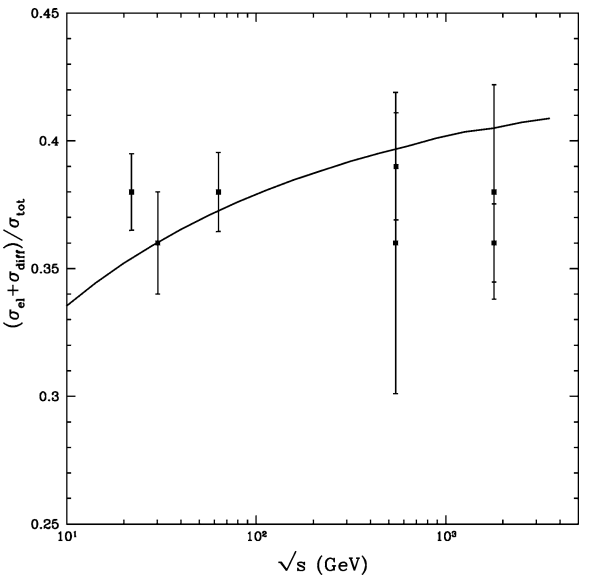

(b)

Fig. 4. For $\bar{p}p$ scattering; (a) elastic cross-section (b) the ratio R_D. Data compilation from Refs. [16,18].

is exponential). It is this Gaussian shape of the profile function which produces a cross-section with a $\ln(\frac{1}{x})$ dependence. We have shown that taking a "dipole" behaviour in the t representation we would have a profile function $S(b) \sim \frac{b}{R} K_1(\frac{b}{R})$, and the resulting cross-sections would asymptotically have a $\ln^2(\frac{1}{x})$

dependence. A reflection of this fact is that the energy dependence of the cross-section (see dashed line of Fig. 2) is much steeper, which is more in accord with the data. Since the original fit to the DIS F_2 data was made with a Gaussian profile in b space, for consistency one should redo the fit with a different profile. This is a task for the future. We summarize our main results:

- We obtain a reasonable value of the total cross-sections;
- The predicted energy increase is too moderate. Both the value of the cross-section and the energy dependence depend on the assumed b-dependence of the profile function. For illustration we have compared with the saturation model of [2]: because of the sharp cutoff in b built into this model, the energy dependence is even weaker. This emphasizes the need to improve, in all saturation models the b-shape of the profile function;
- The difference between σ_{K^+p} and $\sigma_{\pi p}$ at high energy needs an explanation, which cannot be answered within the framework of our model;
- The slow increase of the slope B, is the result of having an almost black disc picture for dipole–proton scattering [20] and not a consequence of a particular form for the b-profile;
- $R_D = \frac{\sigma_{\text{elastic}}+\sigma_{\text{diff}}}{\sigma_{\text{tot}}}$ tends to $\frac{1}{2}$, which is the black disc limit. We reproduce the experimental values for this ratio, which we consider as a success of the model.

In general the approach works better than one would expect, even in the region of long distances. The results obtained are not very sensitive to the input parameters of the projectile hadron, namely, the wavefunction and the parameter Q_0^2. Our use of the saturation models has some predictive power, provided we have enough information about projectile wave function.

Nevertheless, there are serious shortcomings in applying the dipole picture with the concept of saturation to hadronic cross-sections. The crucial feature seems to be the b-dependence of the dipole cross-section which needs further investigation. On a more fundamental level, it is not clear at all, how to relate the dipole picture to the additive quark model: at present these two approaches look almost orthogonal to each other.

Acknowledgements

We would like to thank Claude Bourrely and Jacques Soffer for their help in sending us their files of the cross-section data. We thank Eran Naftali for useful remarks. Two of us (E.G. and E.L.) thank the DESY Theory Division for their hospitality. This research was supported in part by the BSF grant # 9800276, and by the GIF grant # I-620-22.14/1999, and by the Israel Science Foundation, founded by the Israeli Academy of Science and Humanities.

Appendix A

Our results can be easily checked in the asymptotic limit where we have (for simplicity of argument the following discussion is presented at some fixed $r_\perp$, while $r_\perp$ integrations are implicitly assumed):

$$\sigma_{Mp} = 2\pi \int^{b_0^2(x)} db_\perp^2 = 2\pi b_0^2(x), \tag{A.1}$$

where $b_0^2(x)$ is a result of our ansatz on the $b_\perp$ behaviour viz.

$$\sigma_{\text{dipole}-p}(r_\perp, x; b_\perp) = 2\big(1 - e^{-\Omega/2}\big) \tag{A.2}$$

with

$$\Omega = \ln\big[1 - N(r_\perp, x; b_\perp = 0)\big] e^{-\frac{b_\perp^2}{R^2}}.$$

$b_0^2(x)$ can be calculated from the equation

$$\frac{\Omega(r_\perp, x; b_\perp = b_0(x))}{2} = 1,$$

i.e.,

$$b_0^2(x) = R^2 \ln\left[\frac{1}{2}\ln\big(1 - N(r_\perp, x; b_\perp = 0)\big)\right],$$

where $\sigma_{\pi p}^{\text{tot}} = 2\pi b_0^2(x)$ and $\sigma_{pp}^{\text{tot}} = 4\pi b_0^2(x)$. The factor 2 between the cross-sections is due to the fact that we have two dipoles in the proton and one in the meson.

The elastic slope is given by Eq. (4.3)

$$B' = \frac{b_0^4(x)/2}{2b_0^2(x)} = \frac{b_0^2(x)}{4}. \tag{A.3}$$

The energy dependence of B' can now be calculated

$$\frac{dB'}{d\ln(1/x)} = \frac{1}{4}\frac{db_0^2(x)}{d\ln(1/x)} = \frac{1}{16\pi}\frac{d\sigma_{pp}^{\rm tot}(x)}{d\ln(1/x)}.$$

From this formula it is clear that we have an increase of B with $\frac{1}{x}$ which is slower than that of $\sigma_{pp}^{\rm tot}(x)$, and obviously not in accord with the experimental data. Though the above argument was presented for the Gaussian profile, similar conclusions would be obtained for an alternative profile function.

References

[1] ZEUS Collaboration, Eur. Phys. J. C 7 (1999) 609;
ZEUS Collaboration, Phys. Lett. B 487 (2000) 53.

[2] K. Golec-Biernat, M. Wüsthoff, Phys. Rev. D 59 (1999) 014017.

[3] J. Bartels, K. Golec-Biernat, H. Kowalski, Phys. Rev. D 66 (2002) 014001.

[4] E. Gotsman, E. Levin, M. Lublinsky, U. Maor, hep-ph/0209074, Eur. Phys. J. C., in press.

[5] L.V. Gribov, E.M. Levin, M.G. Ryskin, Nucl. Phys. B 188 (1981) 555;
L.V. Gribov, E.M. Levin, M.G. Ryskin, Phys. Rep. 100 (1983) 1.

[6] A.H. Mueller, J. Qiu, Nucl. Phys. B 268 (1986) 427;
J.-P. Blaizot, A.H. Mueller, Nucl. Phys. B 289 (1987) 847.

[7] L. McLerran, R. Venugopalan, Phys. Rev. D 49 (1994) 2233;
L. McLerran, R. Venugopalan, Phys. Rev. D 49 (1994) 3352;
L. McLerran, R. Venugopalan, Phys. Rev. D 50 (1994) 2225.

[8] Ia. Balitsky, Nucl. Phys. B 463 (1996) 99;
Yu. Kovchegov, Phys. Rev. D 60 (2000) 034008.

[9] A. Donnachie, P.V. Landshoff, Nucl. Phys. B 244 (1984) 322;
A. Donnachie, P.V. Landshoff, Nucl. Phys. B 267 (1986) 690;
A. Donnachie, P.V. Landshoff, Phys. Lett. B 296 (1992) 227;
A. Donnachie, P.V. Landshoff, Z. Phys. C 61 (1994) 139.

[10] E.M. Levin, M.G. Ryskin, Phys. Rep. 189 (1990) 267.

[11] A. Kovner, U.A. Wiedemann, Phys. Rev. D 66 (2002) 034031;
A. Kovner, U.A. Wiedemann, Phys. Rev. D 66 (2002) 051502;
A. Kovner, U.A. Wiedemann, hep-ph/0208265;
A. Kovner, U.A. Wiedemann, hep-ph/0207335.

[12] E. Ferreiro, E. Iancu, K. Itakura, L. McLerran, Nucl. Phys. A 710 (2002) 373.

[13] M. Froissart, Phys. Rev. 123 (1961) 1053;
A. Martin, Scattering Theory: Unitarity, Analitysity and Crossing, in: Lecture Notes in Physics, Springer-Verlag, Berlin, 1969.

[14] H.G. Dosch, E. Ferreira, A. Krämer, Phys. Rev. D 50 (1994) 1992.

[15] G.G. Simon, et al., Z. Naturforsch. A 35 (1980) 1;
S.R. Amendola, et al., Nucl. Phys. B 277 (1986) 168;
S.R. Amendola, et al., Phys. Lett. B 178 (1986) 435.

[16] Particle Data Group, D.E. Groom, et al., Eur. Phys. J. C 15 (2000) 1.

[17] G.A. Schuler, T. Sjöstrand, Phys. Rev. D 49 (1994) 2257.

[18] K. Goulianos, Phys. Rep. C 101 (1983) 169.

[19] J. Pumplin, Phys. Rev. D 8 (1973) 2899.

[20] E. Gotsman, E. Levin, U. Maor, Phys. Rev. D 60 (1999) 094011.